Left Ventricular Volume Calculation Using a Count-Based Ratio Method Applied to First-Pass Radionuclide Angiography

Rami A. Gal, Raymond P. Grenier, Steven C. Port, Duncan S. Dymond and Donald H. Schmidt

Cardiovascular Disease Section, University of Wisconsin Medical School, Milwaukee Clinical Campus and Sinai Samaritan Medical Center, Milwaukee, Wisconsin

Most count-based radionuclide methods for calculating left ventricular volume rely on measurement of radioactivity in a peripheral blood sample and a measurement of ventricle to collimator distance. We have developed a method which requires neither a blood sample nor a distance measurement and which is applicable to first-pass radionuclide angiography. The parameters used to calculate volume are the area of pixel, the total counts in the left ventricle and the maximum pixel count. The equation was used to calculate the volumes in 50 patients who had both resting first-pass radionuclide angiography (25 patients with a single crystal and 25 patients with a multicrystal camera) and contrast ventriculography on the same day. Correlation coefficients for end-diastolic and end-systolic volumes showed r ranging 0.93–0.98 and standard error of estimate ranging 23–35 ml for end-diastolic volume (14%–17% of mean end-diastolic volume) and 16–23 ml for end-systolic volume (18%–21% of mean end-systolic volume). Image processing software for extracting the needed values is generally available on most commercial nuclear medicine imaging systems and the additional time for the calculations is short. Although the theory is based on multiple assumptions, the volume calculation appears to be reasonably accurate and clinically applicable.

J Nucl Med 1992; 33:2124–2132

First-pass radionuclide angiography (FPRNA) is used to noninvasively evaluate left ventricular (LV) function. A good correlation between the results of FPRNA and contrast ventriculography has been demonstrated for the measurement of LVEF (*1–6*). Absolute LV volume has been measured from FPRNA studies using geometric methods (*7–9*), count-based methods (*10,11*), and a method that combines geometric and count-based techniques (*9*). Inherent problems with these methods include assumptions about chamber shape in geometric approaches, and the need to correct for attenuation in count-based methods.

Received Mar. 24, 1992; revision accepted Jul. 1, 1992.

For reprints contact: Rami A. Gal, MD, Sinai Samaritan Medical Center, 945 N. 12th St., Milwaukee, WI 53233.

We recently described a simple method for measuring LV volume from gated equilibrium radionuclide angiography data (*12*) that does not require consideration of chamber size or attenuation. In this study, we will show that the same approach (namely, the constant of eccentricity count method) can be successfully applied to first-pass data using either a multicrystal or a single-crystal gamma camera. A discussion of the theory, along with validation from empirical data, is presented in the Appendix.

MATERIALS AND METHODS

Patients

Fifty randomly selected patients (41–77 yr), who were referred for cardiac catheterization during a 12 mo period for clinical reasons (i.e., chest pain, shortness of breath, etc.), underwent rest FPRNA prior to contrast left ventriculography. Their clinical characteristics are listed in Table 1. To determine whether the camera system would affect results, 25 patients were studied using a multicrystal camera and 25 patients were studied using a single-crystal camera.

Gamma Camera Hardware

Multicrystal Camera. A camera with a 14 × 21 array of crystals and a 6 × 9 inch field-of-view (System Seventy-Seven, Baird Corporation) equipped with a 1.5 inch thick parallel-hole collimator was used. The matrix size was 14 × 21 pixels, with a center-to-center pixel spacing of 1.11 cm. The energy window was 140% ± 30% keV.

Single-crystal Camera. A fully digital, small field-of-view (7⅞ inch diameter) portable camera (APEX 215, Elscint, Inc.) equipped with a high-sensitivity, medium-resolution, parallel-hole collimator was used. The matrix size was 32 × 32 pixels, with a center-to-center pixel spacing of 0.635 cm. The energy window was 140% ± 15% keV.

First-Pass Radionuclide Angiography

Data Acquisition. All patients were studied at rest in the supine position. A 1.25 inch, 20-gauge teflon catheter was placed in an external jugular vein in 13 patients. The remaining 37 patients had a 1.75 inch, 18-gauge teflon catheter placed in an antecubital vein. The gamma camera detector was placed over each patient's chest in a 20° to 30° right anterior oblique (RAO) projection after which 1 mCi of ^{99m}Tc-DTPA was injected in order to determine proper positioning. Then, a 25 mCi bolus of ^{99m}Tc-DTPA in less than 1 ml of saline was loaded into an extension tube attached

TABLE 1
Clinical Characteristics

	Single-crystal	Multicrystal	p value
Number of patients	25	25	—
Mean age (y)	61.2	60.7	NS
Males/Females	22/3	18/7	NS
Heart rate (bpm)	68 ± 16	70 ± 13	NS
Diagnosis			
CAD	21	20	NS
VHD	2	3	NS
IDC	2	0	NS
Normal	0	2	NS

CAD = coronary artery disease, VHD = valvular heart disease and IDC = idiopathic dilated cardiomyopathy.

to a catheter. The radionuclide bolus was flushed through this catheter with 20 ml of normal saline.

Acquisition was started just prior to injecting the radionuclide. Counts were accumulated in frame mode for 30 sec using a frame time of 0.03 sec. Data were acquired onto a hard disk and, subsequently, transferred to a floppy disk or magnetic tape for storage and later processing. The two interpreters of the study results (one interpreter for multicrystal and the other for the single crystal camera) were unaware of the contrast ventriculographic results.

Data Processing: Multicrystal Gamma Camera. Each frame of raw data for the entire study was temporally smoothed. The data were then replayed in 1.5 sec intervals as a series of 12 images, each being the sum of 50 individual 30-msec frames. The LV phase was identified to select a region of interest (ROI) over the left ventricle. A time-activity curve was generated by displaying the counts per 30 msec or 60 msec frame within the LV ROI. Peri-ventricular ROI (i.e., a 2-cm wide ring) was chosen to completely surround and be contiguous with the fixed LV ROI, thus incorporating the proximal aorta and the atrium. The average counts per pixel in the ring-shaped background ROI during end-diastole was used to represent the average background per pixel over the LV ROI.

After correcting for background, the computer searched the LV time-activity curve and reported the following data: end-diastolic (ED) and end-systolic (ES) frame numbers for every valid beat, the number of beats used, the heart rate, the total duration of the LV phase in seconds, and the first and last frames of the LV phase. LVEF was then calculated using raw ED counts (EDC), raw ES counts (ESC), and the contiguous-ring background counts (BKG) as follows:

$$\text{LVEF} = \frac{\text{EDC} - \text{ESC}}{\text{EDC} - \text{BKG}}.$$

At this point, LV end-diastolic volume could be calculated using the constant of eccentricity count method algorithm described in detail in the Addendum. The total counts of the entire LV phase were summed into one frame. The sum of all LV phase activity was used to get larger total number of counts (leading to greater precision of measurement) than could be obtained from using only diastolic counts, and generated an "average" LV volume for the entire cardiac cycle.

$V = 1.8\ (Tc/Nmax - 3.5)^{1.5}$, where V is the average volume, 1.8 is a calculated constant, Tc is the total counts in the LV-Roi, Nmax is the maximum pixel count, 3.5 is the intercept of the best fit at 0 volume.

A constant, $k = Tc/V$ may now be used in order to find the volume of the left ventricle at end-diastole, EDV, as follows:

$$\text{EDV} = \frac{\text{EDC}}{k},$$

where EDC equals total counts/sec at end-diastole.

Finally, stroke volume (SV) is calculated from the definition of LVEF as SV = EDV × LVEF. End-systolic volume (ESV) is determined from the formula ESV = EDV − SV.

Single-crystal Gamma Camera. We previously described a method to calculate LVEF from FPRNA data using a single-crystal camera (*13*). Now, using the constant of eccentricity count method, end-diastolic volume can also be calculated.

Briefly, individual 0.03 sec frames are grouped to form 0.5 sec frames in order to visualize the entire LV phase of the study. Then, using the digitized R wave of the electrocardiogram to identify end-diastole, the original 0.03 sec frames within the LV phase are cyclically added to create a crude, uncorrected representative cycle. A nine-point, spatially-smoothed ED frame from that representative cycle is used to manually draw an LV ROI. The latter is used to create a time-activity curve for the entire 30 sec study. From that time-activity curve, the beginning and end of the LV phase are again identified and a frame prior to the LV phase is chosen for subsequent background correction.

The ED and ES frames from the LV phase are automatically identified by the computer according to sequential peak and trough counts. The program also provides automatic beat rejection based on R-R interval criteria and manual beat editing. The latter allows changes in the selection of ED and ES frames based on frame counts, frame images, and the time-activity curve, as well as allowing changes in the determination of the total number of beats accepted or rejected.

A summed background frame is created from a number of frames equal to the number of beats in the representative cycle starting with the previously identified pre-LV phase frame. The ED frame of the representative cycle is subtracted from the summed background frame leaving a background mask. The count ratio between the background frame and the ED frame (counting only masked areas) is used to calculate the background washout factor, which is then used to "normalize" the background frame (*13*).

In order to create the final representative cycle, the ED and ES frames of the accepted beats are summed. Systolic and diastolic frames are aligned according to the average systolic and diastolic intervals as described before (*13*). By adding or condensing frames (an average of two neighboring frames), the final aligned representative cycle always has the correct ED and ES frames, whereas intermediate frames may be slightly modified. The normalized background frame, corrected by the washout factor, is then subtracted from each frame of the representative cycle. After background correction and application of a median filter, a Fourier phase analysis of the aligned representative cycle is performed. The previously drawn LV ROI is then applied to the ED image of the corrected representative cycle and to the LV phase image. At this point, the operator adjusts the LV ROI, if necessary, to conform to the borders of the phase image. If the LV ROI is adjusted, the entire beat selection process is repeated using the new ROI. LVEF is calculated from the final background corrected representative cycle as:

$$\text{LVEF} = \frac{\text{ED counts} - \text{ES counts}}{\text{ED counts}}.$$

On the ED frame of the representative cycle (which is not corrected for background radiation activity), a ring background ROI (1-in pixel wide) is placed around the LV ROI. The average counts per pixel in the former ROI are then subtracted from the latter. Total counts in the left ventricle in the ED frame are calculated. The background-corrected representative cycle is then summed and total LV counts and the maximal pixel count in the LV ROI are measured. The end-diastolic volume is then calculated using the same six equations that were used to calculate volume from data obtained with a multicrystal camera. Likewise, stroke volume and end-systolic volume can be calculated using this EDV and the previously calculated LVEF.

Contrast Ventriculography

Left heart catheterization and coronary arteriography were performed using a standard Judkins or Sones technique. Contrast ventriculography was performed at 30 frames/sec in the 30° RAO and left anterior oblique (LAO) projections using 30–50 ml of diatrizoate meglumin (Renografin 76(R)). LV volumes and EF were calculated using the biplane area-length method described by Kennedy et al. (*14*). Only sinus beats were selected. Three experienced interpreters were unaware of the FPRNA results.

Statistical Methods

Paired observations were analyzed using a Student's t-test and a least squares fit for determination of a regression equation. The significance of difference was determined at the $p < 0.05$ level.

RESULTS

All 50 patients had good quality contrast ventriculographic and radionuclide angiographic studies. The patients were divided into two groups: 25 patients who had FPRNA using a multicrystal camera and 25 patients who were studied using a single-crystal camera.

Contrast Ventriculography

The average heart rate was 69 ± 15 bpm with no significant difference between the two groups of patients. Coronary arteriography revealed severe coronary artery disease (≥ 70% diameter narrowing in one or more vessels) in 41 of the 50 patients. Of the remaining patients, five had valvular heart disease (mitral valve prolapse in two, rheumatic mitral valve disease in one, and aortic valve disease in two), two patients had idiopathic dilated cardiomyopathy and two patients had no signs of heart disease.

Radionuclide Angiography Counting Statistics

Multicrystal Camera. A 25 ± 2 mCi tracer bolus resulted in 184,163 ± 37,311 cps during the right ventricular phase. An average of 7 beats (range 4–12 beats) were included in the representative cycle. The average heart rate during the study was 70 ± 13 (p = ns compared with heart rate during contrast ventriculography).

Single-crystal Camera. The same average amount of tracer resulted in 140,015 ± 23,812 cps during the right ventricular phase. An average of 6 beats (range 5–8 beats) comprised the representative cycle. The average heart rate during the study was 68 ± 16 (p = ns compared with the mean heart rate during contrast ventriculography).

Ejection Fraction

The contrast LVEF ranged from 11% to 87%, whereas LVEF obtained by FPRNA ranged from 15% to 87% (Table 2).

Multicrystal Camera. For the 25 patients who had their FPRNA study done using a multicrystal camera, the mean contrast LVEF was 53% ± 23%, whereas the FPRNA LVEF was 54% ± 23% (p = ns). Comparing contrast LVEF with FPRNA LVEF, linear regression analysis yielded a correlation coefficient of 0.98 and a s.e.e. of 5%.

Single-crystal Camera. For the 25 patients undergoing FPRNA using a single-crystal camera, the mean contrast LVEF was 55% ± 21%, whereas the mean FPRNA LVEF was 54% ± 18% (p = ns). Linear regression analysis revealed a correlation coefficient of 0.94 and a s.e.e. of 7%.

Volumes

Contrast ventriculographic EDV and ESV ranged from 94–453 ml and from 12–353 ml, respectively. The FPRNA EDV and ESV ranged from 65–469 ml and from 12–365 ml, respectively.

Multicrystal Camera. The mean contrast values for EDV and ESV in these 25 patients were 162 ± 57 ml and 87 ± 67 ml, respectively, whereas calculations using the FPRNA data revealed a mean EDV and ESV of 150 ± 62 ml and 81 ± 68 ml, respectively (p = ns). The correlation coefficient for EDV was 0.93, with a s.e.e. of 23 cc (which was 14% of the average EDV). For ESV, the correlation coefficient was 0.98, with a SEE of 16 cc (which was 18% of the mean ESV) (Fig. 1).

Single-crystal Camera. The mean contrast ventriculographic EDV and ESV were 210 ± 92 ml and 110 ± 97 ml, respectively. The corresponding FPRNA calculations revealed a mean EDV and ESV of 202 ± 88 ml and 104 ± 87 ml, respectively (p = ns). For EDV, the correlation coefficient was 0.93, with a s.e.e. of 35 cc (17% of the mean EDV). For ESV, the correlation coefficient was 0.97, with a SEE of 23 cc (21% of the mean ESV) (Fig. 2).

DISCUSSION

Radionuclide angiographic blood-pool studies are well suited to the measurement of LV volumes. Several investigators have reported their findings with these techniques compared with contrast ventriculography. Two general approaches have been used: count-based (nongeometric) and combined geometric and count-based methods. Geometric techniques require accurate spatial resolution of the left ventricle. This is best accomplished in the RAO projection where the left ventricular long axis can be measured. In contrast, a count-based method is less dependent on geometric models or on precise spatial resolution, and does not require that studies be done in the

TABLE 2
Left Ventricular Volume Measurements

Single-crystal camera							Multicrystal camera						
	LVEF (%)		EDV (ml)		ESV (ml)		Patient	LVEF (%)		EDV (ml)		ESV (ml)	
Patient no.	RNA	CV	RNA	CV	RNA	CV	no.	RNA	CV	RNA	CV	RNA	CV
1	74	69	127	171	33	53	26	77	71	98	112	28	32
2	77	92	135	151	31	12	27	84	80	84	96	14	19
3	22	22	469	453	365	353	28	65	62	144	131	50	49
4	74	84	144	135	37	21	29	23	17	233	211	181	175
5	50	51	164	176	82	86	30	15	11	321	300	273	267
6	63	65	146	129	53	45	31	29	32	283	258	201	174
7	68	65	174	176	55	61	32	30	29	206	215	145	152
8	41	49	222	202	131	103	33	37	38	176	236	111	146
9	19	25	346	412	280	311	34	65	55	110	129	39	58
10	58	62	65	94	27	36	35	60	55	156	180	62	81
11	64	58	94	120	34	50	36	87	87	115	124	14	17
12	71	77	141	183	40	43	37	76	74	100	98	24	28
13	68	60	146	108	46	44	38	59	56	159	160	65	71
14	63	60	158	165	58	66	39	81	74	113	122	22	32
15	42	37	279	256	161	161	40	87	87	95	119	12	16
16	20	16	289	364	231	306	41	77	76	72	118	16	28
17	50	52	155	122	77	59	42	68	67	96	96	31	32
18	68	78	141	147	45	32	43	68	68	151	181	49	58
19	25	17	279	251	209	209	44	41	39	196	212	115	129
20	39	34	273	305	166	202	45	34	35	160	203	106	132
21	60	65	198	211	78	74	46	34	39	129	109	85	67
22	68	63	261	175	83	64	47	14	21	199	233	171	184
23	52	45	207	208	99	114	48	39	30	139	157	86	110
24	55	54	235	249	105	116	49	63	71	105	130	39	38
25	62	84	213	218	81	35	50	38	45	134	134	82	74
Mean ± s.d.	54 ± 18	55 ± 21	202 ± 88	210 ± 92	104 ± 87	110 ± 97		54 ± 23	53 ± 23	150 ± 62	162 ± 57	81 ± 68	87 ± 67
s.e.e.	7		35		23			5		23		16	
p	ns		ns		ns			ns		ns		ns	
r	0.94		0.93		0.97			0.98		0.93		0.98	

CV = contrast ventriculography, EDV = end-diastolic volume, ESV = end-systolic volume, LVEF = left ventricular ejection fraction and RNA = first-pass radionuclide angiography.

RAO projection. A count-based method is also well suited for serial studies, which allow the evaluation of the effects of interventions. However, when using a count-based method, factors such as background activity, tissue attenuation, and self-attenuation of activity within the blood pool must either produce negligible effects or have a constant predictable effect in order for radionuclide volumes to correlate closely with contrast ventriculographic volumes.

Previous count based volume measurements have used assumed attenuation coefficients and either measured or estimated distances between the center of the LV and the collimator (*10,15*). Furthermore, blood sampling has been used to establish the counts/volume relationship (*11*).

Previously, count-based methods were used primarily with the gated technique because it provided higher counting statistics and better resolution than could be achieved with the first-pass approach. We also recently presented a count-based method for gated blood-pool studies (*12,16*). This current study presents a count-based method for first-pass studies based on the same principles as those for gated studies, but with some changes made to suit the first-pass approach. This latter method is based on two important principles:

1. Average LV volume is calculated using all the frames in the LV phase, which increases the counting statistics and creates a more spherical LV shape and, consequently, less eccentricity.
2. Two constants have been added. The first constant depends upon the average LV volume, which is based on the summed LV phase (as noted above), and the other originates from the characteristics of the gamma camera (i.e., the pixel size).

This method is fast and easy to use. Software for extracting the needed values exist on most commercial gamma cameras and provide the end result (i.e., end-diastolic volume) within seconds. The necessary variables include total counts and maximal pixel counts in the LV ROI, the parameters of the ring background ROI around the left ventricle, background-corrected ED counts, the number

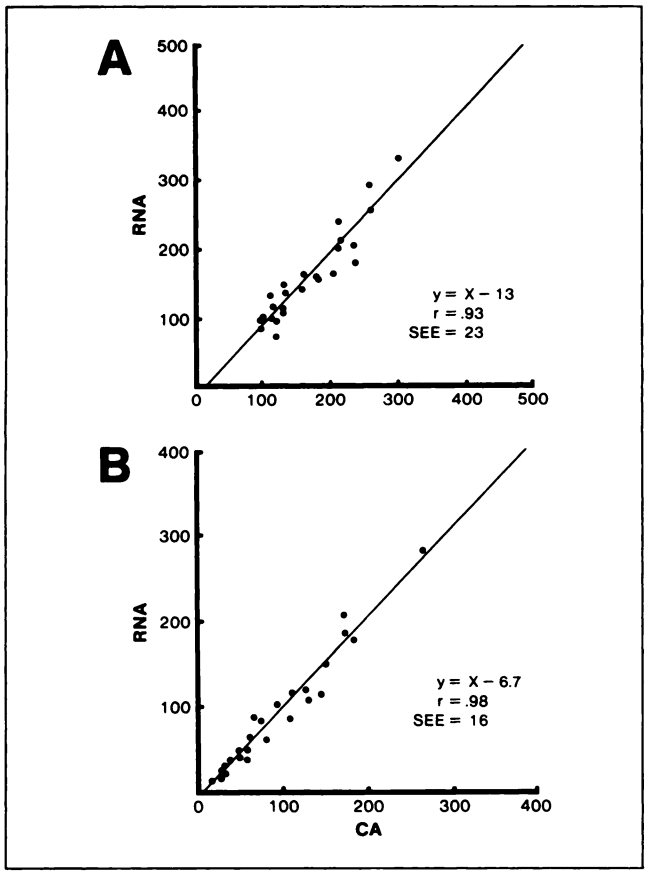

FIGURE 1. Multicrystal gamma camera. Linear regressions between left ventricular volumes by contrast angiography (CA) and radionuclide angiography (RNA) at end-diastole (A) and end-systole (B).

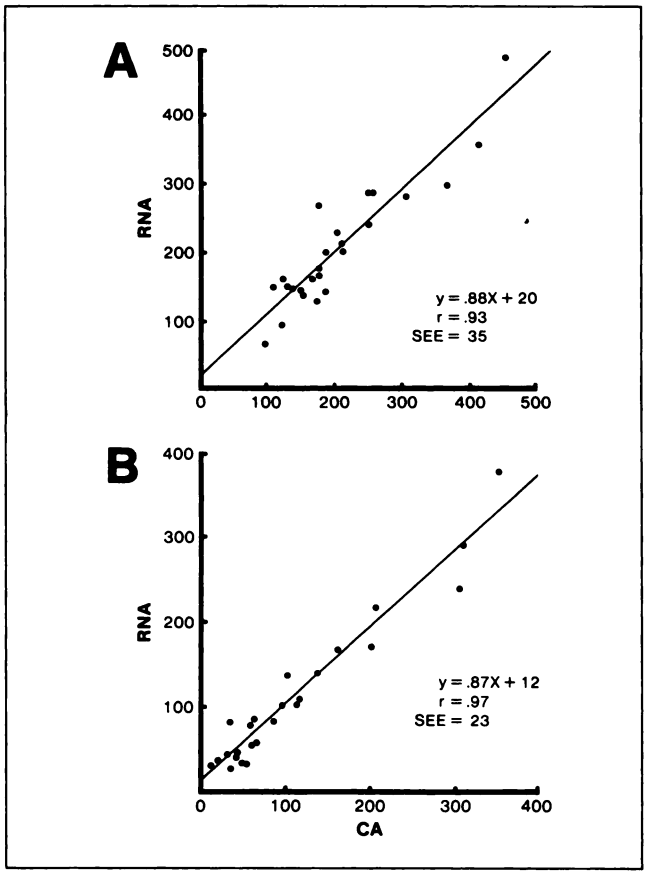

FIGURE 2. Single-crystal gamma camera. Linear regressions between left ventricular volumes by contrast angiography (CA) and radionuclide angiography (RNA) at end-diastole (A) and end-systole (B).

of beats used during acquisition, the frame time and the pixel size.

End-systolic volume should not be calculated directly by this method because the background-corrected counts in end-systole are sometimes too low. This appears to be the problem only in patients with very small ESV. Therefore, the best way to calculate this volume is from the values of EDV and EF (which was assessed prior to the EDV calculation) using a method that was previously described (*13,17*). This method gave good results for both the multicrystal and the single-crystal gamma cameras. Correlation coefficients for EDV and ESV were between 0.93 and 0.98, and the s.e.e. ranged from 23 to 35 cc for EDV (14%–17% of mean EDV) and from 16 to 23 cc for ESV (18%–21% of mean ESV). These results compare favorably with the results of other investigators (*8–10*).

Clinical Implications

Lately, new isonitrile agents were introduced to the cardionuclear field for assessment of both LV function and myocardial perfusion. With these tracers the LV function can be evaluated by first-pass RNA. Subsequently, the interest in first-pass studies has increased. The methods for assessment of LVEF and regional motion is well established. The proposed method of volume calculation complements the assessment of LV function in our institution and seems to correlate well in clinical studies. Although the theory is based on multiple assumptions, the method does not require distance measurement, complicated manual attenuation correction or blood samples. The volume measurement is easy to obtain with an image processing software that is available on most commercially used nuclear medicine systems. It adds only a short time to the processing time.

APPENDIX

COUNT-BASED METHOD THEORY AND EMPIRICAL VALIDATION

In this addendum, we will support our theory that LV volume can be calculated using count data alone obtained from first-pass radionuclide angiography. It will also be shown that by using data from the sum of the LV phase, higher counts can be obtained (which improves the accuracy of the calculation) and a more spherical shape of the ventricle is produced (which reduces the effect of eccentricity). Furthermore, it will be shown that the average volume of a pulsating ellipsoidal chamber conforms to exactly the same algorithm as a resting chamber. Finally, we introduce a method to calculate the distance between the colli-

mator face and the mid-plane of the left ventricle to account for differences in this distance in patient studies.

DEVELOPMENT OF THE EQUATIONS FOR A COUNT-BASED METHOD TO CALCULATE LV VOLUME

Hypothesis: The Volume of a Sphere Can Be Determined Using Only Count Data

If a spherical balloon is filled with a radioactive tracer, the total counts (T_c) observed with the gamma camera will be proportional to the volume of the sphere (V) in ml, such that in the absence of attenuation:

$$T_c = kV, \qquad \text{Eq. A1}$$

where k is the proportionality constant in counts/ml.

In addition, the maximum pixel count (N_{max}) will be proportional to the product of the volume elements, a (which is the balloon diameter in cm) times S (which is the cross-sectional area of the pixel in cm^2) such that:

$$N_{max} = kaS, \qquad \text{Eq. A2}$$

where k is the same proportionality constant in counts/ml as in Equation A1 as proven by in vitro experiment with balloons filled with uniform concentration of ^{99m}Tc. The experiment showed linear correlation between observed counts and the true volume of balloons in the range of 34–394 m, thus verifying that intra-volume scatter in the balloons completely compensated for attenuation losses in this range of volumes. The unknown quantity, k, can thus be eliminated by dividing Equation A1 by Equation A2 to form the ratio, R:

$$R = \frac{T_c}{N_{max}} = \frac{kV}{kaS} = \frac{V}{aS}. \qquad \text{Eq. A3}$$

By using the equations to calculate the volume of a sphere and the cross-sectional area of a sphere, $\frac{V}{a}$ in Equation A3 can also be written as $\frac{2}{3}$ A. Therefore, substituting $\frac{2}{3}$ A for $\frac{V}{a}$ in Equation A3 shows that R can be written as follows:

$$R = \frac{2}{3}\frac{A}{S} \text{ or } A = 3/2\ SR. \qquad \text{Eq. A4}$$

Equation A4 indicates that the cross-sectional area of a sphere, A, is directly proportional to the count-based ratio, R. In this equation, S is the area of a square whose sides are the center spacing between crystals in a multicrystal camera or between pixels in a single-crystal or Anger camera. S is a fixed function of the collimator design or pixel matrix and can be determined experimentally for each collimator and camera system (see Hypothesis C). Thus, Equation A4 is essentially nongeometric because the area is obtained directly from counts and from the value of the center-to-center spacing between pixels of the gamma camera.

The count method becomes analogous to classical methods for LV volumes by substituting 3/2 SR for A in all formulas. The volume of a sphere can, thus, be expressed in terms of the cross-sectional area of the sphere, A, as follows.

By again using the equations to calculate the volume of a sphere and the cross-sectional area of a sphere, volume can also be written as:

$$V = 0.75A^{3/2} \qquad \text{Eq. A5}$$

Then, by combining Equations A4 and A5, the volume of a sphere can, also, be expressed as a function of R, namely:

$$V = 1.38S^{3/2}R^{3/2} \qquad \text{Eq. A6}$$

Using Equation A6, the volume of a sphere can be obtained directly from count data alone since V is simply a function of the measured quantities of R (which is the ratio of T_c/N_{max}) and S, which is known for the specific gamma camera system used.

Hypothesis: The Volume of an Ellipsoid Can Be Determined Using Only Count Data

Because the left ventricle approximates the shape of an ellipsoid rather than a sphere, Equation A5 needs to be modified for the volume of an ellipsoid of revolution, V_e, whose cross-section is an ellipse with an eccentricity, e, where $e = \frac{a^2 - b^2}{a^2}$, and where a is the long-axis and b is the short-axis of the ellipsoid. After solving for e, the volume formula of $V = 0.75A^{3/2}$ can be expressed for an ellipsoid as:

$$V_e = 0.75(1 - e^2)^{1/4}A^{3/2}. \qquad \text{Eq. A7}$$

Again, by substituting 3/2 SR for A in Equation A7, V_e can be expressed as a function of R as follows:

$$V_e = 1.38(1 - e^2)^{1/4}S^{3/2}R^{3/2}. \qquad \text{Eq. A8}$$

Equations A7 and A8, used to calculate the volume of an ellipsoid of revolution, are the same as Equations A5 and A6 used to calculate the volume of a sphere where the eccentricity is equal to 0. Equation A7 is used extensively in invasive angiography to calculate LV from a measurement of the ventricular silhouette area, A, and the length of the long-axis, L. Indeed, Equation A7 is identical to the classical formula, $V = 0.85\ A^2/L$, in the Dodge-Sandler approach (*18*), since it can be shown that $0.75\ (1 - e^2)^{1/4} = 0.85\ A/L$. Due to the high spatial resolution of contrast angiography, the area can be determined very accurately by planimetry, but this is not the case with radionuclide angiography. Equation A7 also expresses the important mathematical fact that the determination of the volumes of ellipsoids of revolution having the same eccentricity and is a function only of the cross-sectional area, A. It will be shown that these conditions are matched closely by the left ventricle at end-diastole in the RAO view.

Equation A8, which uses the values of S and R to calculate A, constitutes the theoretical basis for the constant eccentricity count method for determining volumes using only count data obtained from first-pass radionuclide angiography studies. Instead of using planimetry, which is severely limited by spatial resolution in radionuclide angiography, this nongeometric technique uses the study's high-count resolution to determine R of total counts to the maximum pixel count, which is proportional to A. Contrast ventriculographic studies done in 30 patients have shown that the mean eccentricity of the left ventricle is 0.77 ± 0.07 at end-diastole and that the mean eccentricity of the average LV volume throughout the cardiac cycle is 0.61 ± 0.1. When the eccentricity value at end-diastole is applied to Equation A8, we find that the volume formula for the left ventricle can be expressed as:

$$V_e = 1.38(1 - 0.77^2)^{1/4}S^{3/2}R^{3/2} \qquad \text{Eq. A9}$$

which equals

$$V_e = 1.38(0.8)S^{3/2}R^{3/2}.$$

Therefore, LV volume obtained from end-diastolic count data in the RAO view would overestimate the volume by 20% if the shape of a sphere is assumed.

Hypothesis: The Value of S Is a Fixed Instrumentation Constant That Can Be Determined for Any Gamma Camera System

It is important to establish that the quantity, S, is a fixed instrumentation constant and not itself a function of volume. This can be achieved most accurately by an experimental verification of Equation A6, which allows the calculation of spherical volume from count data alone. The hypothesis is discussed in detail in previous papers (*12,16*).

EMPIRICAL DETERMINATION OF THE NONGEOMETRIC CONSTANT ECCENTRICITY VOLUME ALGORITHM

Because the shape of the left ventricle is best approximated by an ellipsoid of revolution, we used a set of ellipsoidal balloons to evaluate our theory of constant eccentricity. This shape is difficult to achieve because even thick-walled balloons become more spherical as the volume is increased, which causes the eccentricity to decrease. Consequently, a set of four ellipsoidal balloons was used in order to cover the desired range of eccentricity and volume. The average eccentricity of the balloons was 0.6.

The count measurements of the four balloons were used to determine the basic count-to-volume algorithm pertinent to the multicrystal camera's 1.5-inch thick collimator configuration. Each balloon was oriented with its major axis parallel to the face of the collimator to simulate the RAO view used in radionuclide and contrast left ventricular angiography. The mid-plane of the balloon was maintained at a 3-inch distance from the collimator face. The results of plotting the actual volume, V_{actual}, versus the ratio, R, of T_c/N_{max}, are shown in Figure 1. A least-squares best fit to the data is shown as a solid line in Figure A1.

The equation for the solid line is as follows:

$$V_{calc} = 1.8(R_3 - 3.5)^{1.5}, \qquad \text{Eq. A10}$$

where V_{calc} is the volume calculated from the least-squares fit and $R_3 = T_c/N_{max}$, measured at 3 inches from the collimator. The constant, 3.5, is the intercept of the best fit curve at zero volume, reflecting the fact that a point source with negligible volume still yields an R value greater than one, which is due primarily to finite spatial resolution for very small volumes.

Figure A2 shows the plot of calculated volume, (V_{calc}), using Equation A10 versus actual measured volume, V_{actual}. The regression and correlation coefficients are 1.03 and 0.998, respectively. The s.e.e. is 5.9 ml, which represents the lower limit of error for this constant eccentricity count method. The results in Figure A clearly verify that accurate volumes can be obtained from count data for ellipsoids of revolution.

DETERMINATION OF THE AVERAGE VOLUME OF A PULSATILE BALLOON

In order to determine whether measurements made with balloons can approximate the beating heart, we also calculated the volume of pulsatile balloons. The balloons were kept stationary during each step of the filling phase. This allowed us to carefully measure the balloon's volume at each filling step in order to simulate an average volume for a volume that continuously changes, such as in the cardiac cycle. The balloons were then pulsed continuously and volumes were measured with each pulsation. There was a minimal volume increase of 100 ml over 4 to 7 equal filling steps, with equal time intervals between steps. The average volume, V, was calculated as the mean of the actual volumes of all the filling steps during one pulsation, and the corresponding ratio, R, for each pulsation was obtained from the sum of the frames of data of all the filling steps. The average volume, V_{actual}, plotted versus R_3 is shown in Figure A3. The regression analysis is identical to that obtained in Figure A1 for the resting balloons.

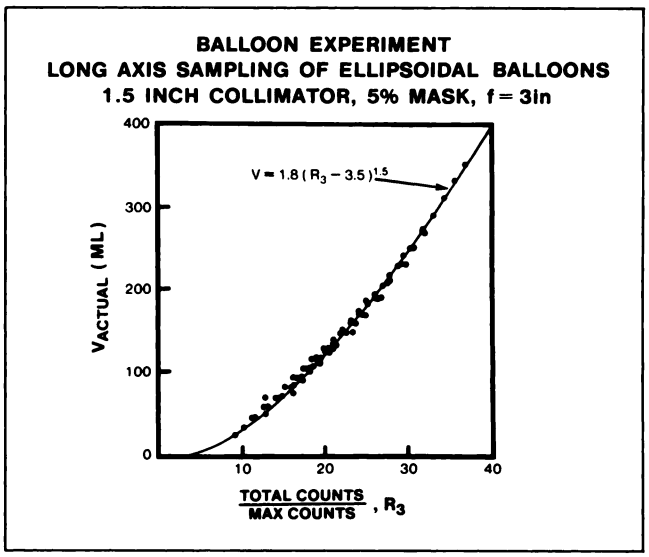

FIGURE A1. Plot of actual volume in ml versus the ratio, R_3, of total observed counts to maximum pixel counts measured at 3 inches from the 1.5-inch collimator. The solid circles are observed data. The solid line is a best least squares fit to the data.

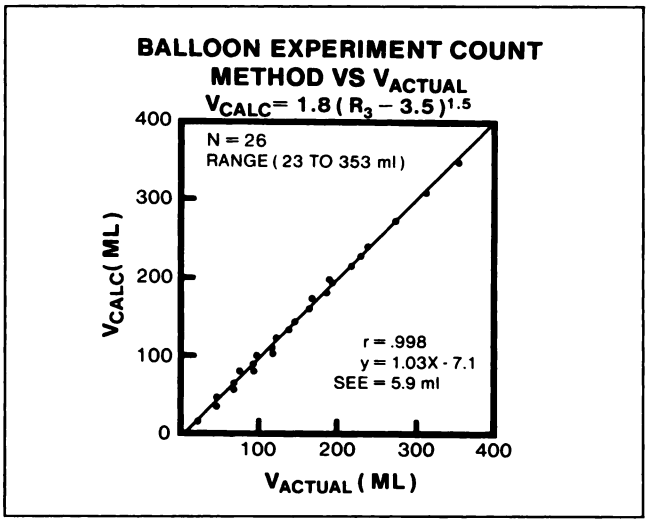

FIGURE A2. Solid circles are balloon volumes calculated from Equation A10 versus actual volumes in ml. Solid line is linear least squares best fit to the data. These data shows excellent agreement between the count method and actual volume.

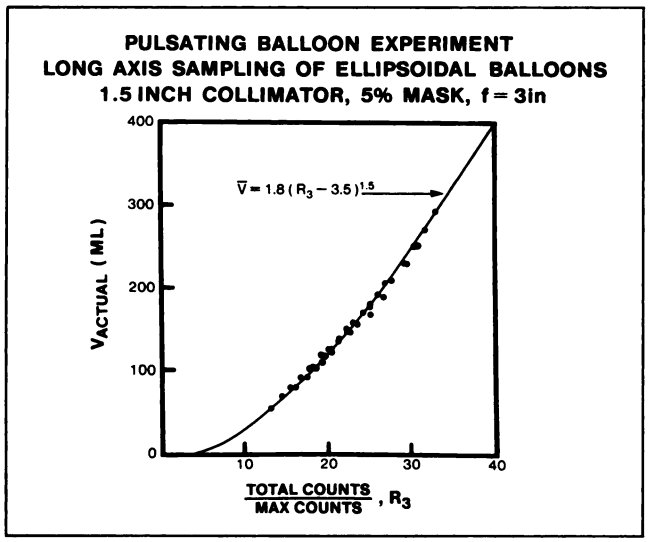

FIGURE A3. The solid circles are a plot of the actual average volume of pulsating balloons versus the R value obtained by summing the total counts and maximum pixel counts from each volume step during the pulsation. The solid line is a plot of Equation A10 developed from stationary balloon measurements showing that Equation A10 is valid for pulsatile volumes.

The solid line in Figure A3, which represents the best fit, is the identical curve of Equation A10. This experiment shows that the sum of the entire cardiac cycle can be used as a reference volume in LV volume studies rather than using only the short counting interval at the time of end-diastole. Therefore, higher counts, at a factor of about 30, become available to accurately determine the ratio, R, for calculating the average volume of the left ventricle using Equation A10 in first-pass radionuclide angiography studies. The average LV volume is obtained from summing the data of the entire cardiac cycle (the LV phase).

In addition to providing higher counts, an average left ventricular volume obtained from all frames in the LV phase from a study performed in the RAO view takes on a more spherical shape, i.e., it has an eccentricity approaching zero, than the more ellipsoidal shapes projected by end-diastolic or end-systolic volumes. The eccentricity of the average LV volume can be determined from RAO silhouettes drawn at equal time intervals throughout the entire cardiac cycle. As indicated earlier, measurements made in 30 patients who also underwent RAO contrast ventriculography, yielded an eccentricity of 0.61 ± 0.1 for the average LV volume. Hence, balloons with an eccentricity of 0.6 are a proper match for the determination of LV volume in the RAO view. Thus, Equation A10 can be used to determine the average volume of the LV phase, and LV eccentricity does not need to be considered in this calculation. Once V is determined in ml, the proportionality constant, k, in counts/ml can be obtained using Equation A1; i.e., $k = V_{calc}/T_c$. End-diastolic volume can then be obtained by applying Equation A1 to the background-corrected total counts observed at end-diastole; i.e., $EDV = T_c/k$.

EFFECT OF DISTANCE FROM THE COLLIMATOR

Total counts, T_c, and the maximum pixel count, N_{max}, are both functions of the distance, f, between the mid-plane of a balloon and the face of the collimator. The dependence of R on f was evaluated by balloon measurements placed between 1 and 7 inches in 1-inch steps from the face of the collimator. Three balloons with volumes of 100, 150 and 230 ml were measured at each of these seven distances. The ratio, R_3/R_f, which is the value of R at 3 inches to the value of R at f inches, was plotted against distance, f, in Figure A4. The solid line in this figure is the least-squares best fit to the data. The equation for the regression line is as follows:

$$R_3 = (1.07 - 0.024f)R_f, \qquad \text{Eq. A11}$$

where R_3 is the ratio, T_c/N_{max}, at a 3-inch distance from the collimator face (which is needed to calculate volume using Equation A10), f is the distance in inches from the collimator face to the mid-plane of the balloons, and R_f is the ratio of T_c/N_{max} observed at an f distance. Equation A11 shows that if f is known, the equivalent value of R at 3 inches, R_3, can be calculated. The distance between the collimator and the mid-plane of the left ventricle in an RAO view is typically in the range of 5 to 7 inches. Using Equation A11, these distances result in R_3/R_f values of 0.95 for R_3/R_5 and 0.90 for R_3/R_7. Therefore, if a 5-inch distance between the collimator and the mid-plane of the left ventricle is assumed, a maximum error of 5% in R_3 can occur.

However, as noted, in order to calculate R_3 we need to know the distance, f, from the chest to the mid-ventricle. A technique to estimate this distance in an RAO view is available from unpublished data, developed by Nickel, Schad, and coworkers, using data obtained from computerized tomographic scans and contrast ventriculography. Using the weight and height of the patient, they developed a relationship for distance as follows:

$$f = 7.8\,\frac{W}{H}, \qquad \text{Eq. A12}$$

where f is the chest to mid-ventricle distance in inches, W is body weight in kg and H is height in cm. Verification of Equation A12 was obtained in our catheterization laboratory in 28 patients. Using biplane contrast ventriculography, the average measured chest to mid-plane distance in these patients was 5.1 ± 0.75 inches. Using Equation A12, the average distance was 5.1 ± 0.4 inches.

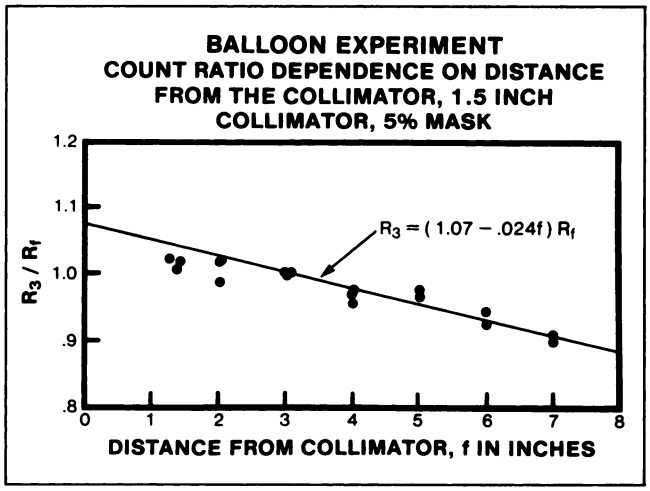

FIGURE A4. Variation of the ratio R versus distance, f, in inches from the 1.5-inch collimator. The data shown as solid circles were obtained with three balloons of 100, 150 and 230 ml. The value of R at a 3 inch distance is normalized to unity.

The serial application of Equations A3, A12, A11, A10 and A1 constitutes the nongeometric constant of eccentricity count method algorithm for determining left ventricular volumes from count data obtained in the RAO view in a first-pass radionuclide angiography study.

$$R_f = \frac{T_c}{N_{max}} \qquad \text{Eq. A3}$$

$$f = 7.8\,\frac{W}{H} \qquad \text{Eq. A12}$$

$$R_3 = (1.07 - 0.024f)R_f \qquad \text{Eq. A11}$$

$$V_{calc} = 1.8(R_3 - 3.5)^{1.5} \qquad \text{Eq. A10}$$

$$T_c = kV, \text{ which equals } k = \frac{T_c}{V_{calc}} \qquad \text{Eq. A1}$$

After solving for k, end-diastolic volume (EDV) can be calculated from the background-corrected counts in end-diastole (EDC), again using Equation A1 as:

$$EDV = \frac{EDC}{k}.$$

Stroke volume (SV) is then calculated using this value for EDV and the calculated value for ejection fraction (LVEF) as SV = EDV × LVEF. End-systolic volume (ESV) is then calculated as ESV = EDV − SV.

ACKNOWLEDGMENTS

The authors thank Lorna Grade for editorial assistance and Jean Kaiserling and Lori Roesch for secretarial assistance.

REFERENCES

1. Schelbert HR, Verba JW, Johnson AD, et al. Nontraumatic determination of left ventricular ejection fraction by radionuclide angiocardiography. *Circulation* 1975;51:902–909.
2. Hecht HS, Mirell SG, Rolett EL, Blahd WH. Left-ventricular ejection fraction and segmental wall motion by peripheral first-pass radionuclide angiography. *J Nucl Med* 1978;19:17–23.
3. Marshall RC, Berger HJ, Reduto LA, Gottschalk A, Zaret BL. Variability in sequential measures of left ventricular performance assessed with radionuclide angiocardiography. *Am J Cardiol* 1978;41:531–536.
4. Bodenheimer MM, Banka VS, Fooshee CM, Hermann GA, Helfant RH. Quantitative radionuclide angiography in the right anterior oblique view: comparison with contrast ventriculography. *Am J Cardiol* 1978;41:718–725.
5. Jengo JA, Mena I, Blaufuss A, Criley JM. Evaluation of left ventricular function (ejection fraction and segmental wall motion) by single pass radioisotope angiography. *Circulation* 1978;57:326–332.
6. Dymond DS, Elliott A, Stone D, Hendrix G. Spurrell R. Factors that affect the reproducibility of measurements of left ventricular function from first-pass radionuclide ventriculograms. *Circulation* 1982;65:311–322.
7. Sullivan RW, Bergeron DA, Vetter WR, et al. Peripheral venous scintillation angiocardiography in determination of left ventricular volume in man. *Am J Cardiol* 1971;28:563–567.
8. Scholz PM, Rerych SK, Moran JF, et al. Quantitative radionuclide angiocardiography. *Cathet Cardiovasc Diagn* 1980;6:265–283.
9. Massie BM, Kramer BL, Gertz EW, Henderson SG. Radionuclide measurement of left ventricular volume: comparison of geometric and counts-based methods. *Circulation* 1982;65:725–730.
10. Nickel O, Schad N, Andrews EJ, Fleming JW, Mello M. Scintigraphic measurement of left ventricular volumes from the count-density distribution. *J Nucl Med* 1982;23:404–410.
11. Schneider RM, Jaszczak RJ, Coleman RE, Cobb FR. Disproportionate effects of regional hypokinesis on radionuclide ejection fraction: compensation using attenuation-corrected ventricular volumes. *J Nucl Med* 1984;25:747–754.
12. Massardo T, Gal R, Grenier RP, Schmidt DH, Port SC. Left ventricular volume calculation using a count based ratio method applied to multigated radionuclide angiography. *J Nucl Med* 1990;31:450–456.
13. Gal R, Grenier RP, Carpenter J, Schmidt DH, Port SC. High count rate first-pass radionuclide angiography using a digital gamma camera. *J Nucl Med* 1986;27:198–206
14. Kennedy JW, Baxley WA, Figley MM, et al. Quantitative angiocardiography. The normal left ventricle in man. *Circulation* 1966;34:272–278.
15. Yang KT, Thompson CJ, Mena I. Automatic ventricular edge detection for determination of left ventricular volumes, ejection fraction and regional ejection fractions from first pass radioisotope angiography. *Comput Med Imaging Graph* 1988;12:147–158.
16. Grenier R, Port SC. Geometric methods for determining left ventricular volume [Letter]. *J Nucl Med* 1991;32:552–555.
17. Gal R, Grenier RP, Schmidt DH, Port SC. Background correction in first-pass radionuclide angiography: comparison of several methods. *J Nucl Med* 1986;27:1480–1486.